ground water

Stream-Stage Response Tests and Their Joint Interpretation with Pumping Tests

by Tobias S. Rötting[1,2], Jesus Carrera[2], Jose Bolzicco[2], and Josep Maria Salvany[2]

Abstract

Hydraulic head response to stream-stage variations can be used to explore the hydraulic properties of stream-aquifer systems at a relatively large scale. These stream-stage response tests, also called flooding tests, are typically interpreted using one- or two-dimensional models that assume flow perpendicular to the river. Therefore, they cannot be applied to systems that are both horizontally and vertically heterogeneous. In this work, we use the geostatistical inverse problem to jointly interpret data from stream-stage response and pumping tests. The latter tests provide flow data (which are needed to resolve aquifer diffusivity into transmissivity and storage coefficient) and may supply supplementary small-scale information. Here, we summarize the methodology for the design, execution, and joint numerical interpretation of these tests. Application to the Aznalcóllar case study allows us to demonstrate that the proposed methodology may help in responding to questions such as the continuity of aquitards, the role and continuity of highly permeable paleochannels, or the time evolution of stream-aquifer interaction. These results expand the applicability and scope of stream-stage response tests.

Introduction

Naturally occurring or controlled stream-stage variations have been used successfully to study large-scale hydraulic properties of fluvial aquifers (e.g., Pinder et al. 1969; Grubb and Zehner 1973; Loeltz and Leake 1983; Carrera and Neuman 1986c; Reynolds 1987; Sophocleous 1991; Tabidian et al. 1992; Genereux and Guardiario 1998; Bolster et al. 2001). Aquifer reaction to tidal fluctuations has also been employed to calculate aquifer parameters (e.g., Erskine 1991; Jha et al. 2003). A large number of one-dimensional (1D) and mostly analytical solutions are available for interpreting the tests (e.g., Ferris 1951; Rorabaugh 1960; Rowe 1960; Hantush 1961; Cooper and Rorabaugh 1963; Pinder et al. 1969; Hornberger et al. 1970; Singh and Sagar 1977; Onder 1997; Mishra and Jain 1999; Zlotnik and Huang 1999; Singh 2003; Swamee and Singh 2003). Some authors have also interpreted the tests in a plane perpendicular to the stream (Loeltz and Leake 1983; Carrera and Neuman 1986c; Moench and Barlow 2000) to account for two-dimensional (2D) heterogeneity.

However, these interpretation methods suffer from three limitations. (1) They assume that flow is perpendicular to the river, thus ignoring heterogeneity (irregular aquifer geometry, paleochannels, silt layers, etc.). (2) They use only head data, which only reveal information about aquifer diffusivity (Carrera and Neuman 1986b). Accurate flow rate data, which are difficult to obtain during high-flow events, are needed to resolve aquifer diffusivity into transmissivity and storage coefficient. (3) They do not allow direct incorporation of other types of hydraulic data (e.g., cross-hole pumping tests). These additional tests can yield the aforementioned flow rate data and supplementary small-scale information. They also create additional flow conditions to better identify the transmissivity distribution ("multi-directional aquifer stimulation": Snodgrass and Kitanidis 1998; "hydraulic tomography": Yeh and Liu 2000, Liu et al. 2002). Joint interpretation of different tests or of different data types provides an integrated picture of the system and can narrow the range of likely parameter sets (e.g.,

[1]Corresponding author: Department of Geotechnical Engineering and Geosciences, Technical University of Catalonia, 08028 Barcelona, Spain; tobias.roetting@upc.es

[2]Department of Geotechnical Engineering and Geosciences, Technical University of Catalonia, 08028 Barcelona, Spain

Received October 2004, accepted July 2005.

doi: 10.1111/j.1745-6584.2005.00138.x

Carrera and Neuman 1986c; Anderman et al. 1996; Weiss and Smith 1998; Saiers et al. 2004). This can be best achieved by automatic calibration of a numerical aquifer model (Poeter and Hill 1997; Hill et al. 1998; Carrera et al. 2005).

When data from several tests are interpreted jointly, some parameters may change between tests (e.g., severe floods may erode streambed sediments, thereby altering stream-aquifer interaction). The flexibility of a numerical model should allow accounting for these changes.

The aim of this article is to summarize a methodology for the design and execution of stream-stage response tests and their joint interpretation with pumping tests. A quasi–three dimensional (3D) geostatistical inversion code is used for parameter estimation. The methodology is illustrated through application to the Aznalcóllar case study. Here, an alluvial aquifer became contaminated by heavy metal–laden acidic water from a mine tailings spill. Pumping tests did not suffice to characterize the aquifer on a sufficiently large scale, so that a number of questions were left unanswered regarding (1) the continuity of a silt layer that was found while building a permeable reactive barrier (PRB) across the floodplain; (2) the role and extent of deep gravel channels; (3) the time evolution of the stream-aquifer connection; and (4) the impacts of the PRB construction. A stream-stage response test was performed to answer these questions.

Methodology

Stream-Stage Response Test Design and Execution

A stream-stage response test is a hydraulic test that consists of observing the head response of an alluvial aquifer to a controlled change of the water level in a stream or channel. This response is measured in piezometers and can be used to determine aquifer characteristics and parameters. As the source of stress is a line and not just a point, the area of influence is much greater than that of pumping tests. The aquifer can be stressed either by raising or by lowering the water level in the stream. The methods presented here can be applied to both kinds of situations.

The three key parameters in the design of a stream-stage response test are (1) the magnitude of water level change in the stream; (2) the test duration; and (3) the measurement intervals. They are discussed subsequently.

Stream stage should change as much as possible to maximize head response, but the water level should remain within the channel (i.e., should not inundate the floodplain) to simplify interpretation. The water level change depends on river channel characteristics and flow rate, which can be specified if the stream-stage variation is generated by opening the gates of a dam.

Appropriate test duration and measurement intervals depend on aquifer parameters. Test duration should be long enough for most wells to react significantly to the stage change (i.e., longer than equilibration time, t_{eq}). Measurement intervals should be short enough to define the transient part of the test (i.e., shorter than the well reaction time, t_r). For planning purposes, t_{eq} and t_r can be approximated for each observation well as (e.g., Crank 1975)

$$t_{eq} \approx \frac{SL^2}{T} \qquad (1)$$

$$t_r \approx 0.1 \frac{SL^2}{T} \qquad (2)$$

where L is the distance between well and stream and T and S are estimates of aquifer transmissivity and storage coefficient, respectively. Ideally, test duration should be longer than the t_{eq} of all the wells involved in the test. Estimates of T and S can be obtained from pumping tests or from textural data and geology. However, room should be left for surprises as deep observation wells may respond faster than derived from Equations 1 and 2 (Carrera and Neuman 1986c) and T may grow with scale (e.g., Sanchez-Vila et al. 1996).

The network of piezometers should cover the whole area of interest. Well screens should be short wherever vertical variations in aquifer parameters or responses are expected. All relevant features (e.g., abrupt lateral changes in aquifer characteristics, formation boundaries, layers) should be monitored. Preliminary information on the approximate position of such boundaries may be obtained from standard hydrogeological exploration methods (boreholes, trenches, geophysical methods, hydraulic tests, etc.) and from the observation and qualitative interpretation of piezometric surfaces under different flow conditions (especially aquifer response to previous stream-stage variations, i.e., flood events, if such data are available).

The river stage should be measured at several points, especially if stream width or section changes along the test reach. In general, the propagation of the hydraulic pulse is much faster in the channel than in the aquifer. However, if the test reach is long, upstream wells close to the river will have equilibrated by the time the pulse reaches the downstream end of the reach. Therefore, it is necessary to measure stream stage along the river. Moreover, actual stage variations are sensitive to river width. Therefore, stage measurement points should be located so as to make sure that river width and section variability are properly sampled.

The test may be performed by recording the response to a naturally occurring flood or to an artificial variation in stream stage (e.g., by opening or closing the gates of a dam). However, Equation 2 implies that measurements may have to be made at short intervals. Continuous recording of heads at such intervals may saturate the recording devices. Therefore, if possible, an artificial stream-stage variation should be preferred. In this way, not only the heads but also other parameters (e.g., concentrations or temperature) may be monitored. Here, we will deal only with head measurements.

Test data are best interpreted in terms of head variations (rather than actual values). Head variations are defined as changes in head caused by the stream-stage response test compared to the natural evolution of heads in the aquifer system, similar to drawdowns in pumping tests. River-stage variations are defined analogously. The advantages of this procedure are explained subsequently. Measurements must start prior to the test in order to be able to filter out natural trends of head variability.

It may be advisable to use automatic recording devices in piezometers and river-stage measuring points, particularly if many points have to be monitored at short intervals.

Numerical Interpretation

Emphasis is placed on estimation of spatially varying parameters. Otherwise (i.e., homogeneous medium), a model perpendicular to the river should suffice. Moreover, many conceptual models need to be tested. Therefore, the use of geostatistical inversion methods is recommended (Meier et al. 2001). This reduces the effort devoted to calibration and allows the modeler to concentrate on conceptual issues. Here, we used the quasi-3D finite-element code TRANSIN II (Medina et al. 1995). This code calculates both direct and inverse flow and transport problems in a stationary or transient regime. The inverse problem is solved by minimizing a maximum likelihood criterion (Carrera and Neumann 1986a), which includes prior information on aquifer parameters. For a geostatistical interpretation, it can include the spatial correlation structure (covariance matrix) of the hydraulic conductivity of the aquifer system. The code also computes several model identification criteria (Akaike, modified by Akaike, Hannan, and Kashyap; details are given by Carrera and Neuman 1986a), which allow one to evaluate the quality of different model structures. According to Carrera and Neumann (1986c), Kashyap's (1982) is the best criterion because it takes into account the goodness of fit while penalizing overparameterization.

The modeling procedure consists of five steps: (1) definition of the conceptual model; (2) definition of a geostatistical model for transmissivity; (3) discretization; (4) nonlinear maximum likelihood estimation of the model parameters; and (5) revision of the conceptual model and repeated calibration until obtaining a good fit between observed and modeled data. The general principles of this methodology have been described by Meier et al. (2001). The details specific to the joint interpretation of stream-stage response and pumping tests with parameters varying in time are described subsequently.

Conceptual Model

To simulate stream-aquifer interaction, a "mixed-type" boundary is used, relating flow across the riverbed to the difference between external head H_e (river stage) and aquifer head h according to:

$$q = \alpha(H_e - h) \tag{3}$$

where q is flux (m/d), i.e., flow rate per unit area, and α is the leakance (d^{-1}), also called conductance, which represents the hydraulic conductivity of the riverbed divided by its thickness. More complex approaches to describe stream-aquifer interaction have been developed (for a review, see Sophocleous 2002). Nevertheless, here we apply this simple approach in order to keep the number of parameters low.

Aquifer heads and stream stage are expressed in terms of variation with respect to the natural evolution of the system. A hydraulic test can be considered as a signal that is added on the natural evolution of the studied system. Therefore, when the test data are expressed in terms of variations, the model only needs to simulate the changes induced by the test (in our case, pumping rates or variations in river stage and their effect on aquifer heads) but not, for example, the natural base flow in the aquifer. This simplifies boundary and initial conditions. Only the boundary conditions that are driving variables of the test (pumping rates, river-stage variations) have to be expressed as time functions. All other boundary conditions of parameters that are not changed by the test are homogeneous (zero values). Initial aquifer head variations and stream-stage variations are also zero because by definition, before the start of the test, aquifer heads and steam stages are equal to the "natural" values of the system. Additionally, systematic measurement bias (e.g., due to erroneous reference levels) is eliminated by working with head variations.

Geostatistical Model for Transmissivity

Transmissivity can be treated deterministically or stochastically. In the latter case, one must specify the covariance structure of transmissivity. In layered aquifers, the different alluvial layers that were deposited at different times can often be assumed as statistically independent of each other. The same applies to any other component of the aquifer (i.e., anthropogenic structures such as PRB). This must be reflected in the covariance matrix, where each formation is represented by a block that describes intercorrelation within the formation or structural unit, while the different blocks are not correlated with each other.

Discretization

In the quasi-3D approach implemented in TRANSIN II, aquifer layers are represented by 2D triangles and rectangles, while aquitards are represented by 1D linear elements. If equilibration time in the aquitard with respect to head changes in the aquifers is quick compared to the duration of the hydraulic tests and time steps of the model, then transient head variations within the aquitard can be neglected and the aquitard can be represented by linear elements. Otherwise, the linear elements have to be refined by intermediate nodes (Chorley and Frind 1978). In order to include both data of small-scale pumping tests and those of larger-scale stream-stage response tests, numerical accuracy demands that the mesh be highly refined between sources of stress (rivers and pumping wells) and observation points. However, the mesh can be coarser far away from these zones.

Different events that occurred during a period where aquifer parameters did not change can be interpreted within the same mesh. To do so, the data sets and time functions of each event have to be separated by "dummy" periods with zero stress that allow aquifer head and stream-stage variations to recover to initial levels (Figure 1).

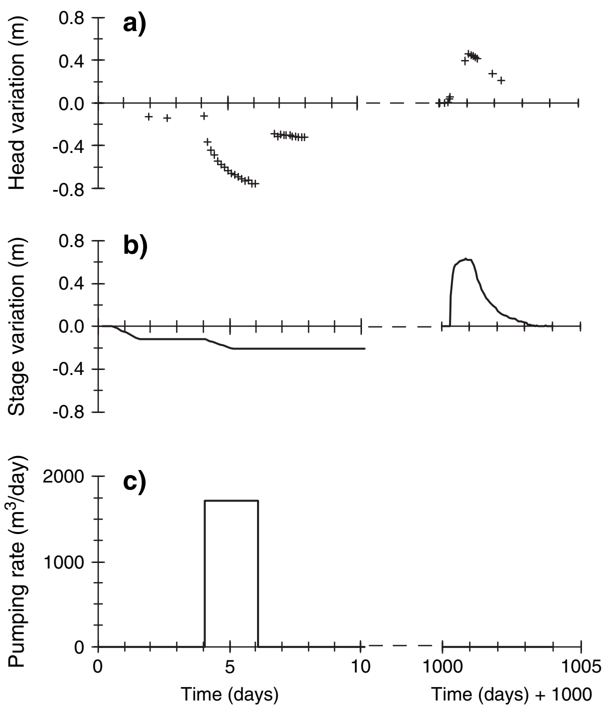

Figure 1. Example of input processing in order to interpret data from one pumping test and one stream-stage response test in one mesh: (a) observed head variations in an observation well ("S-5" of the case study), (b) stream-stage variation, (c) pumping rate of a pumping well ("S-3" of the case study).

Calibration

Calibration is best performed automatically to avoid the need for performing a large number of model runs to attain a manual fit by trial and error. In essence, one has to specify the covariance matrix of all the data. Here, we assume head errors to be independent, so that one only needs to define their standard deviation. As for the model parameters, the covariance matrices of transmissivity are derived from the geostatistical model. All other parameters are assumed independent, so that one only needs to define their standard deviation.

All model parameters (aquifer transmissivities, aquitard hydraulic conductivities, storage coefficients, and leakance) are calibrated simultaneously using the data of all the tests. As a result, the problem may be ill posed, resulting in instability, high uncertainty, and poor convergence. To deal with these problems, one may choose to fix some parameters or to artificially increase the weight assigned to prior estimates. Here, we propose the approach of Carrera and Neuman (1986c), which consists of initially assigning a high weight to prior information in order to facilitate convergence. In successive runs, prior information weight is lowered stepwise in order to give the model more freedom in adjusting parameter values.

When different model configurations are tested in order to explore the structure of the stream-aquifer system, they can be compared using a number of criteria (Carrera et al. 1993). We use residual analysis (examining the fit between measured and computed heads at every observation point) and parameter assessment (evaluating whether computed parameters are reasonable) for preliminary screening of conceptual models. For quantitative comparison, we use overall model fit, as measured by the heads objective function (sum of squared weighed residuals; for details, see Carrera and Neuman 1986a and Meier et al. 2001) and, better, Kashyap's model structure identification criterion (equation 30 in Carrera and Neuman 1986a).

The Aznalcóllar Case Study

Site and Geology

The aim of the Aznalcóllar case study was to characterize the River Agrio alluvial aquifer situated in the Aznalcóllar mining district in the Seville province of southwest Spain (Figure 2a). This aquifer had become contaminated by heavy metal–laden acidic water from the mine tailings spill that occurred on April 25, 1998 (e.g., Grimalt et al. 1999). As one of the remediation measures, a PRB was built across the floodplain (Carrera et al. 2001). As the pit for barrier emplacement was excavated, the aquifer turned out to be more complex than expected (Salvany et al. 2004) in several aspects, which will be explained subsequently.

The River Agrio is a tributary of the River Guadiamar (Figure 2a) and forms an alluvial valley made up of four Quaternary terraces (Salvany et al. 2004):

- The upper terrace (T3) is hydraulically separated from the other terraces by the bedrock and will therefore not be considered in this study.
- The intermediate terrace (T2) forms a wide flat area below the hills. It is composed of three layers (Figure 3): a lower layer of coarse gravels and sands, an intermediate layer of silts containing subordinate levels of sands and small gravels, and an upper layer of sandy gravels, which always lies above the water table and will not be considered hereinafter. The deepest gravels form a lower paleochannel that flows obliquely to the surface terrace and river trends.
- The lower terrace (T1) is a single deposit of sandy gravels a few meters below the T2 terrace. It forms an upper paleochannel that follows the river trend and occasionally cuts the T2 deposits and even the bedrock.
- The current floodplain (T0), 1 to 1.5 m below the T1 terrace, is an erosive terrace that cuts through T1.

The Miocene Blue Marls Formation forms the impervious base of the aquifer system.

To sum up, in the vicinity of the PRB (Figure 3, cross section B-B′), the hydrogeologic system consists of the rivers Agrio and Guadiamar and of three layers: a confined aquifer formed by the lower T2 deposits, an aquitard consisting of the T2 intermediate silts, and a phreatic aquifer formed by T1 deposits. In this study, we suppose that the phreatic aquifer is cut off ~400 m up- and downstream of the PRB because the silt layer outcrops right on top of the Blue Marls in the channel of the River Agrio (crosshatched areas in Figure 2b). In the following, the T1 deposits will be referred to as "upper gravels" and the T2 lower gravels as "lower-layer gravels" or "paleochannel."

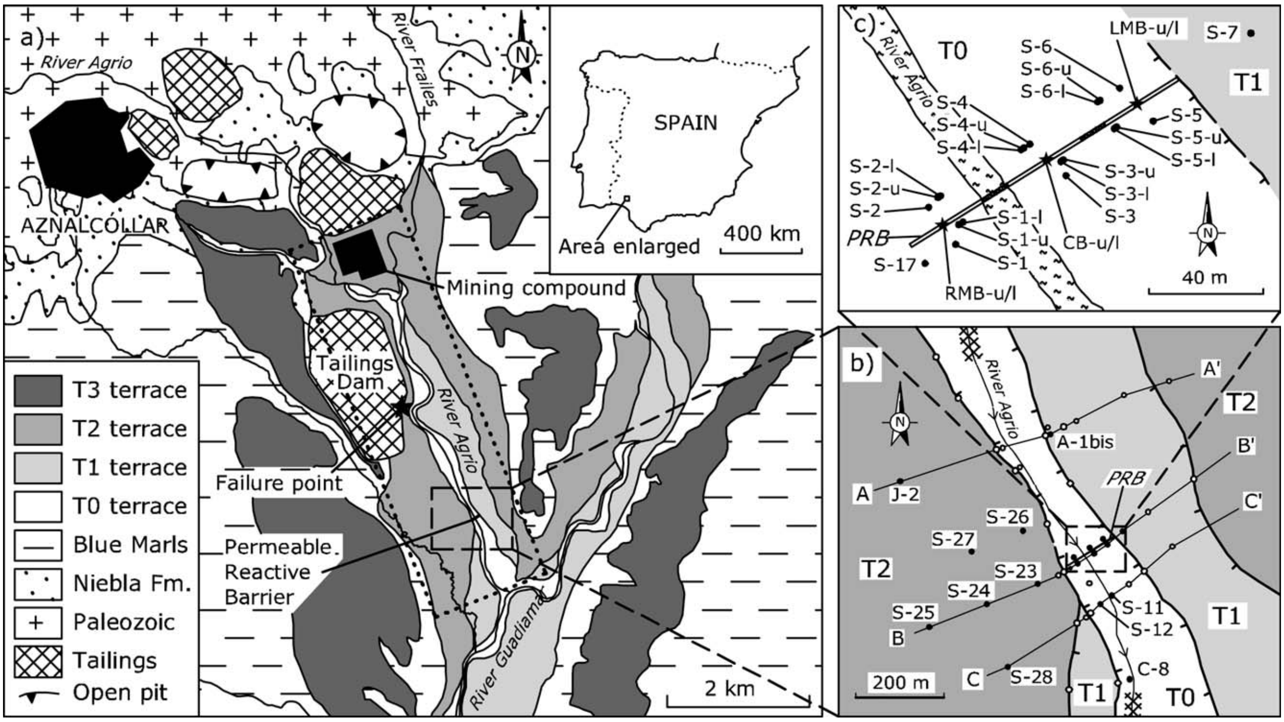

Figure 2. (a) Geological map of the studied site showing the River Agrio terraces and their bedrock. The dotted-line rectangle shows the extent of the numerical model. (b) Location of observation wells used during the flooding test (filled circles) and of other wells and trenches (open circles). The crosshatched areas show where the Blue Marls appear in the bed of the River Agrio (a and b adapted from Salvany et al. 2004). (c) Observation wells around the permeable reactive barrier ("PRB"). Suffixes "-u" and "-l" stand for wells screened only in the upper or lower gravel layer, respectively. The stars represent piezometer nests inside the three reactive PRB modules ("RMB, CB", and "LMB" stand for right margin, central, and left margin barrier module).

The Aznalcóllar PRB spans the floodplain 2 km downstream of the tailings pond. It consists of three reactive modules (Carrera et al. 2001). Each module is 30 m wide, 1.4 m thick, and penetrates into the Blue Marls (on average 6 m deep). The three modules are separated by two 10-m wide nonreactive sections of low permeability.

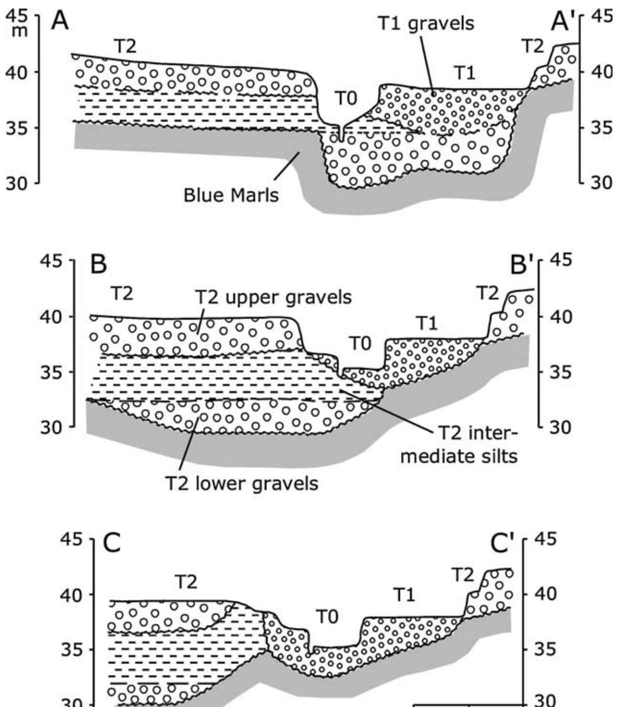

Figure 3. Cross sections of River Agrio deposits (adapted from Salvany et al. 2004). See Figure 2b for location.

Uncertainties remain about the degree of hydraulic connection between the two aquifers and about the lateral extension of the aquifer layers. It is not clear if the silt layer is a continuous feature in the area where the upper gravels overlie the lower gravels. Likewise, the course of the T2 paleochannel is only known in the area where wells have been drilled.

The hydraulic connection of the two aquifer layers to the River Agrio is also unclear: remediation of the toxic spill led to an artificial river channel, which was merely a few meters wide and very shallow. Therefore, it is believed that it was only connected to the upper water table aquifer. However, between December 2000 and January 2001, severe floods reshaped the floodplain morphology, increased the width of the channel to >10 m, and deeply eroded the riverbed. This may have enhanced stream-aquifer interaction between River Agrio and the upper aquifer by changing the hydraulic conductivity of the streambed sediments. The lower aquifer may have also become connected to the upper aquifer and to the river by partial erosion of the silt layer.

As all these features might severely affect PRB efficiency, a number of questions about this hydrogeologic system were raised, regarding (1) the continuity of the silt layer; (2) the geometry of the lower gravel layer and its hydraulic connection to the river; (3) the evolution of stream-aquifer interaction; and (4) the impact of PRB construction on the flow system. A stream-stage response test promised to be an adequate instrument to study these issues.

Stream-Stage Response and Pumping Tests

Prior to stream-stage response test execution, reaction and equilibration time were calculated for several wells in the upper and lower gravel layers using Equations 1 and 2 and prior estimates of *T* and *S* as obtained from pumping tests (see four examples in Table 1). Reaction and equilibration times are quite short, especially for wells in the confined layer. Therefore, automatic sensors were installed in 14 wells and at one point in the river. Due to technical limitations of the data-logging system, the measuring intervals used during the test were somewhat larger than the lowest calculated reaction times (5 min in five wells connected to the water table aquifer, 1 min in all other wells). All other points were measured manually.

The Aznalcóllar drinking water dam was opened at 12:00 h on June 5, 2002 and closed at 12:00 h on June 6, 2002. The flow rate was 11 m^3/s, a value that had produced a large rise in river stage without causing excessive floodplain inundation in previous high-flow events. Water level rose by up to 64 cm near the PRB (Figure 4) and up to 97 cm in a narrow part of the riverbed near well A-1bis (not shown). The evolution of water levels was monitored in 54 wells (Figures 2b and 2c) and at 11 river-stage measurement points. Manual measurements were continued until the evening of June 7; the automatic sensors kept on measuring in 15-min intervals until July 22. Almost all the wells in the floodplain and beneath the T2 terrace responded very quickly (within <1 h) to changes in the river stage.

Prior to the stream-stage response test, three series of cross-hole pumping tests had been performed at the PRB site. Wells S-1, S-3, and S-6 (cf. Figure 2c) were pumped sequentially in each series, and drawdowns were measured in the surrounding wells. Two such series were performed prior to PRB construction (in January and March 2000). They differ somewhat in pumping rates and duration. One test series (in March 2001) was performed after PRB construction and after the riverbed had been affected by the winter 2000/2001 floods. During this last test series, the stream stage of the River Agrio varied twice due to changes in the water release rate of the Aznalcóllar drinking water dam, so this undesired variation had to be taken into account for the interpretation of the test (cf. Figure 1a).

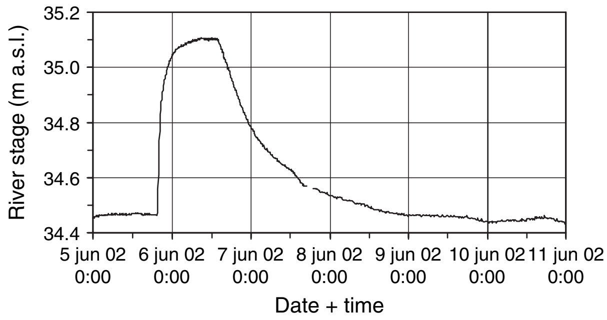

Figure 4. River Agrio stage close to the PRB during the stream-stage response test.

Numerical Interpretation

The numerical model simultaneously interprets the stream-stage response test and the three series of cross-hole pumping tests.

Conceptual Model

The aquifer system consists of two aquifer layers (Figures 3 and 5a) separated by a silt aquitard as described in Site and Geology. The lower confined aquifer consists of the lower gravels in the area of the T2 paleochannel and of T2 intermediate silts in the remaining area between the margins of the alluvial valley. The course of the paleochannel beyond the area where wells had been drilled was extrapolated parallel to the river (Figure 5a). The model area extends up to the mining compound upstream of the PRB (dotted-line rectangle in Figure 1a). Downstream of the PRB, the model boundary is formed by the River Guadiamar. All other boundaries are assumed to be of prescribed flow type and will be treated as no-flow because we are working with head variations (see Methodology).

In order to explore the structure of the aquifer system and to test the benefits of the geostatistical approach, different model configurations were tested. After preliminary screening model runs, three conceptual models were believed reasonable. They differ in leakance zone structure and treatment of transmissivity (geostatistical or deterministic), as summarized in Table 2.

Model 1 contains four leakance zones ("Upstream α," "Upper two-layer α," "Downstream α," "Guadiamar α"; cf. Figure 5b). It assumes that river-aquifer interaction does not change in time. The rivers are hydraulically

Table 1
Estimated Reaction and Equilibration Time for Two Wells in the Upper Gravel Layer and for Two Wells in the Lower Gravel Layer Using Prior Estimates of *T* and *S*

	Upper Gravel Layer (water table aquifer)		Lower Gravel Layer (confined aquifer)	
T (estimated)	300 m^2/d		3000 m^2/d	
S (estimated)	0.2		0.0001	
Well	S-3-u	S-6-u	S-23	S-25
Distance to river (*L*)	7 m	50 m	150 m	400 m
Reaction time (t_r)	5 min	4 h	0.1 min	0.8 min
Equilibration time (t_{eq})	50 min	40 h	1 min	8 min

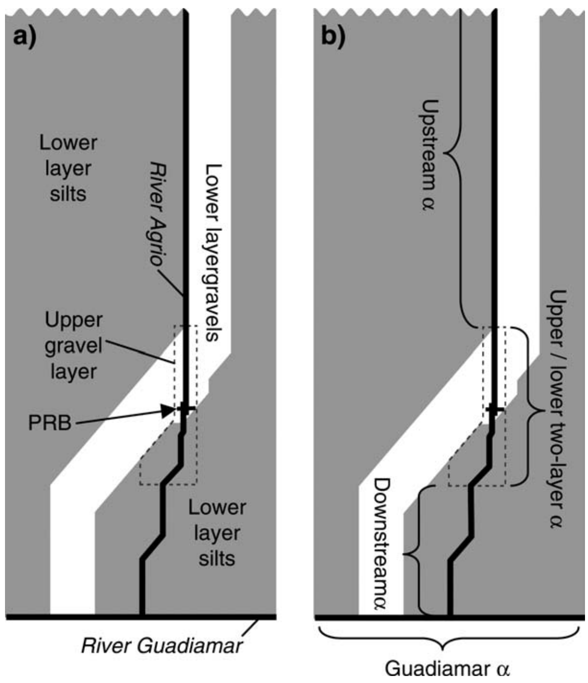

Figure 5. (a) Transmissivity zones (the subdivisions of the geostatistical transmissivity fields are not shown) and (b) leakance zones of the conceptual and numerical model. Only the downstream half of the model area is shown; zones continue homogeneously upstream.

connected only to the uppermost layer in each segment. Therefore, in the two-layer zone, the River Agrio has no hydraulic connection to the lower-layer gravels ("Lower two-layer α" is not assigned).

Model 2 acknowledges that the 2000/2001 floods may have changed the aquifer connection with the River Agrio. This is represented by assigning different leakances to each segment of the River Agrio in the 2000 and 2001/2002 tests. Additionally, the River Agrio may also be connected to the lower layer in the two-layer zone (Lower two-layer α is also assigned in both meshes). River Guadiamar is assumed to remain unchanged by the floods. This totals nine leakances (four leakances for River Agrio in 2000, four leakances for River Agrio in 2001/2002, and one leakance for River Guadiamar, which is identical in both periods).

Model 3 has the same structure of leakance zones as model 2, but in order to examine what is gained by geostatistical inversion, transmissivity is treated deterministically: the transmissivity fields of the upper aquifer layer, the lower aquifer paleochannel, and the three barrier modules are replaced by single zones, resulting in a model with only 11 independent transmissivity zones that are all statistically independent from each other.

As no quantitative data on leakances were available, prior estimates and initial values of all leakances of the three model configurations were set to an intermediate value of 1 d^{-1}. The variances were set to 5 orders of magnitude ($\sigma^2 \log \alpha = 5$) in order to allow the models to assign both very good and very poor hydraulic connections to the different leakance zones.

Discretization

The two aquifer layers are represented by 2D triangles and squares (Figures 6a through 6c). The aquitard is represented by 1D linear elements without intermediate nodes because preliminary evaluation of the equilibration time in the silt aquitard indicated that equilibration is fast. Intermediate nodes are used only at wells with continuous screens that connect both aquifers. These nodes distribute the total pumping rate between the aquifers.

The total model domain is 5120 by 1536 m. The largest 2D elements have a side length of 256 m, the smallest elements, 0.7 m. Close to the PRB, the River Agrio is represented as an area having the real width of the river. Further away it is represented as a line. Stream-aquifer interaction is represented using Equation 3, so that total inflow at each node is equal to the flux, given by Equation 3, times the nodal area. The latter is taken as the length of river represented by the node times a fixed width of 12 m in the portions where the river is represented as a line.

Two unconnected meshes are used for simulating the four tests: one ("2000 mesh") representing conditions prior to the PRB construction and the winter 2000/2001 floods, and one ("2001/2002 mesh") representing conditions after both events. The latter is a bit more refined in order to adequately represent the barrier and the additional wells. Two tests series are interpreted in each mesh. The first test series is separated from the second series by a 1000-d dummy period to allow heads to recover to zero (cf. Figure 1).

Time discretization is variable and was adjusted until further refinement in time did not change the solution.

Table 2
Overview of Tested Model Configurations: Treatment of Transmissivity and Number of Estimated Parameters in the Three Model Configurations

	Model 1	Model 2	Model 3
Treatment of transmissivity	Geostatistical	Geostatistical	Deterministic
Transmissivity zones	102	102	11
Storage zones	4	4	4
Leakance zones	4	9	9
Sum of estimated parameters	110	115	24

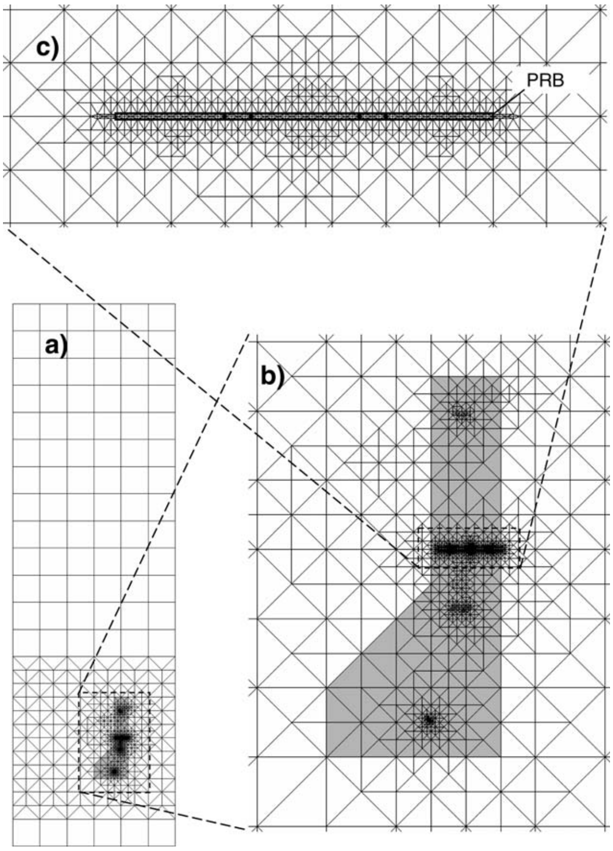

Figure 6. Finite-element mesh in plane view, showing only the 2001/2002 mesh. (a) Total modeled area, (b) zoom of the zone with two layers. In a and b, the two-layer zone with the smaller upper layer is shaded in gray. (c) Zoom of the surroundings of the PRB.

Geostatistical Model for Transmissivity

As stated in the Methodology, the different alluvial layers and each module of the PRB are statistically independent. Prior information about aquifer transmissivities was calculated as saturated layer thickness times an initial estimate of hydraulic conductivity (Table 3) that was obtained from grain size analyses. Saturated thickness was obtained from boreholes and trenches. The silt layer was assumed to be continuous, with a constant thickness of 1 m. From these point values, the transmissivity values were interpolated by block kriging using exponential variograms. The kriging parameters (Table 4) were estimated assuming longer ranges parallel to paleochannels than laterally and choosing relatively short ranges to avoid prior information to force too much continuity.

The transmissivity field of the upper layer has 35 zones, that of the lower aquifer paleochannel has 49 zones, and the lower layer silts are divided into three independent zones. The silt layer is represented by a single zone. For the PRB, each reactive module is divided into four correlated zones, plus two zones for the separating low-permeability modules. This totals 102 transmissivity zones. Each aquifer (cf. Figure 5a) is divided into transmissivity zones that are correlated according to the geostatistical model (cf. Table 4). The size of the zones is adapted according to distance to test zones and density of wells, with zones being smaller where the density of observation points is higher.

Calibration

Standard deviations of head data of the different wells (required for defining the relative weights of head data) were 5 cm for the six fully penetrating wells close to the barrier where the mesh and T zones were refined and 15 cm elsewhere because of increased discretization errors. Pumping well drawdowns were excluded from calibration to prevent discretization and in-well effects such as skin from affecting the aquifer calibration.

Results

Estimated parameters of the three model configurations are represented in Tables 5 and 6. Calibrated heads (Figures 7 and 8) of most wells are shown for model 2, which achieves the smallest residuals (Table 5). Fits are good for most wells during the stream-stage response test (Figures 7 and 8d), except at the end of the recovery period. Fits for the pumping test data are reasonable (Figures 8a through 8c). Since fits are quite similar in the

Table 3
Prior Estimates and Variances of Hydraulic Conductivity (m/d) and Storage Coefficient (−) or Storativity (m^{-1}, for the silt layer) of the Different Model Zones

	Prior Estimate of Hydraulic Conductivity, K (m/d)	Variance or Sill σ^2 of Log T or Log K	Prior Estimate of Storage Coefficient, S (−), or Storativity, S_s (m^{-1})	Variance σ^2 of Log S or Log S_s
Upper gravel layer	200	1[1]	0.2	1
Silt layer	0.05	2	5×10^{-3}	1
Lower-layer gravels	1000	1[1]	10^{-3}	1
Lower-layer silts	0.1	1	10^{-3}	1
Right margin barrier module	0.5	4[1]	0.2	1
Left margin barrier module	1	4[1]	0.2	1
Central barrier module	1	4[1]	0.2	1
Nonreactive sections	0.2	1	0.2	1

[1]Variance for model 3; sill for models 1 and 2, where covariances are determined by block kriging (see text and Table 4).

Table 4
Geostatistical Parameters Used for Block Kriging of the Different Transmissivity Regions of the Model

	Upper Layer	Lower-Layer Gravels (Paleochannel)	Reactive Modules of the PRB
Number of zones	25	49	4 zones/module
Direction of anisotropy (clockwise relative to the river axis near the PRB)	0°	45°	Isotropic
Range in principal direction (m)	100	300	10
Range in secondary direction (m)	30	100	10
Sill ($\sigma^2_{\log T}$)	1	1	4

three PRB modules, only results from the central barrier module are shown. The residuals of model 1 are similar to those of model 2 in most wells as expressed by the heads objective function (Table 5). The major difference can be found in well S-2 during the second pumping test before PRB construction (Figure 9), where model 1 performs much worse than model 2, and model 3 actually achieves the best fit of all models. However, residuals of model 3 are much larger in wells S-3, S-5, S-17 (not shown), and A-1bis (Figure 10). This causes the heads objective function to be more than twice as high as those of the other models. Kashyap's model identification criterion is best (most negative) for model 2 (Table 5). Despite the smaller number of calibrated parameters (cf. Table 2), models 1 and 3 achieve poorer scores.

Calibrated upper-layer transmissivities are similar for models 1 and 2 (Figures 11b and 11c, right-hand side) and generally higher than prior estimates (Figure 11a), except at the upstream end. In the lower-layer paleochannel, the calibrated transmissivities of models 1 and 2 (Figures 11b and 11c, left-hand side) tend to be lower than the prior values, especially close to the southern limits of the displayed area. Toward the northern limits, model 1 assigns transmissivities that are higher than prior estimates, while model 2 assigns lower values. Model 3 calibrates lower transmissivities than the geometric means of models 1 and 2 (Table 5) for both the upper gravel layer and the lower-layer paleochannel. The hydraulic conductivities of the PRB modules in the three models remain similar to their prior estimates (Table 5),

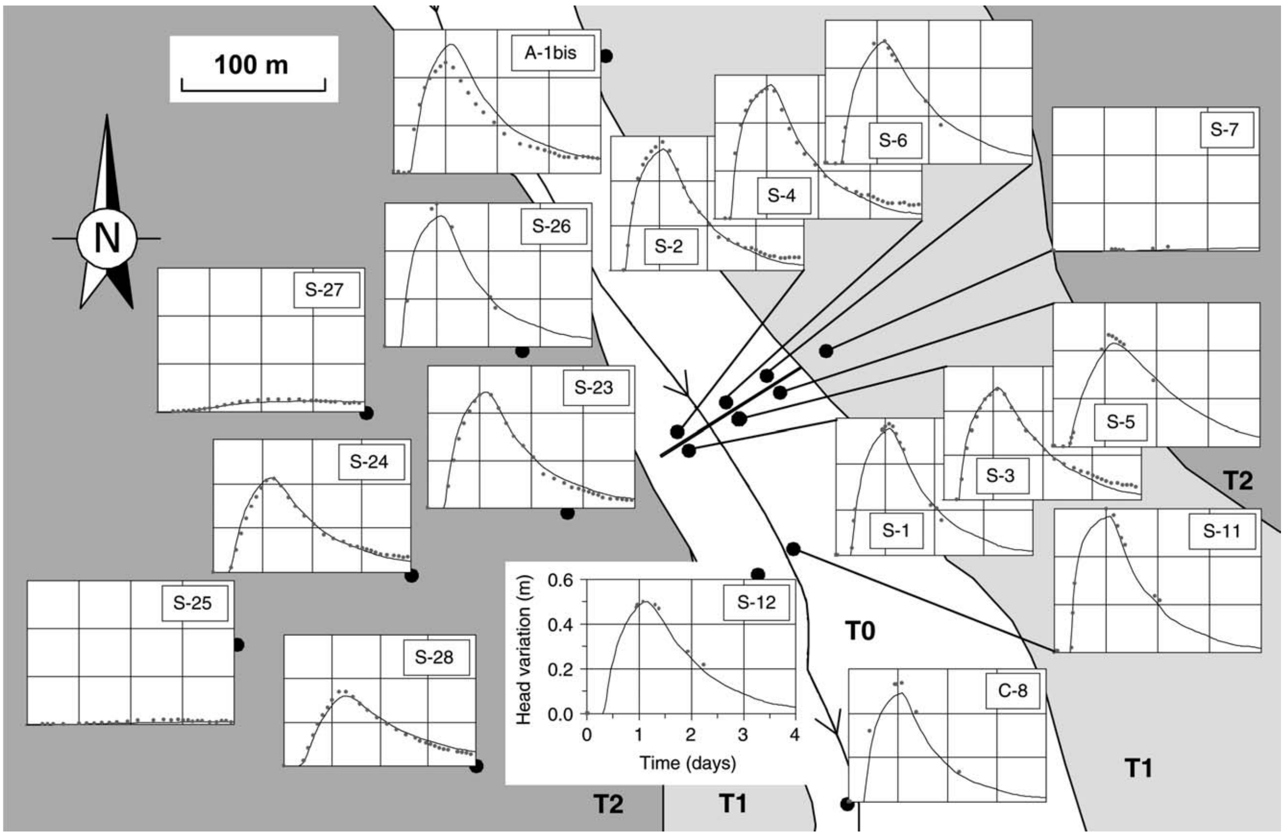

Figure 7. Measured (dots) and calculated (continuous line) head variations of model 2 for the stream-stage response test. For clarity, only selected wells and part of the measured data points are shown.

Table 5
Results of the Model Evaluation Criteria, Prior Estimates and Calibrated Values of Transmissivities (T) of Upper Gravel Layer and Lower-Layer Gravels, Hydraulic Conductivities (*K*) of PRB Modules and Silt Layer, and Storage Coefficients for the Different Model Configurations (for models 1 and 2 geometric mean of each transmissivity field or PRB module)

		Calibrated Values		
	Prior Estimate	Model 1	Model 2	Model 3
Heads objective function	—	224.0	209.5	535.0
Kashyap (1982)	—	−5093	−5209	−4643
Transmissivities and hydraulic conductivities				
Upper gravel layer T (m^2/d)	$166.3 = 10^{2.22}$	$492 = 10^{2.69}$	$416 = 10^{2.62}$	$266 = 10^{2.42}$
Lower-layer gravels T (m^2/d)	$1718 = 10^{3.24}$	$1634 = 10^{3.21}$	$1451 = 10^{3.16}$	$1399 = 10^{3.15}$
Right margin barrier K (m/d)	0.50	0.47	0.46	0.0066
Central barrier K (m/d)	1.0	11	1.1	0.84
Left margin barrier K (m/d)	1.0	1.5	2.2	1.2
Silt layer K (m/d)	0.20	0.066	0.11	0.19
Storage coefficients (−)				
Upper gravel layer	0.20	0.23	0.26	0.20
Silt layer	0.005	0.034	0.049	0.084
Lower-layer gravels	0.001	0.0004	0.0059	0.0011
Lower-layer silts	0.001	0.0007	0.0008	0.0009

[1]For the silt layer: storativity (m^{-1})

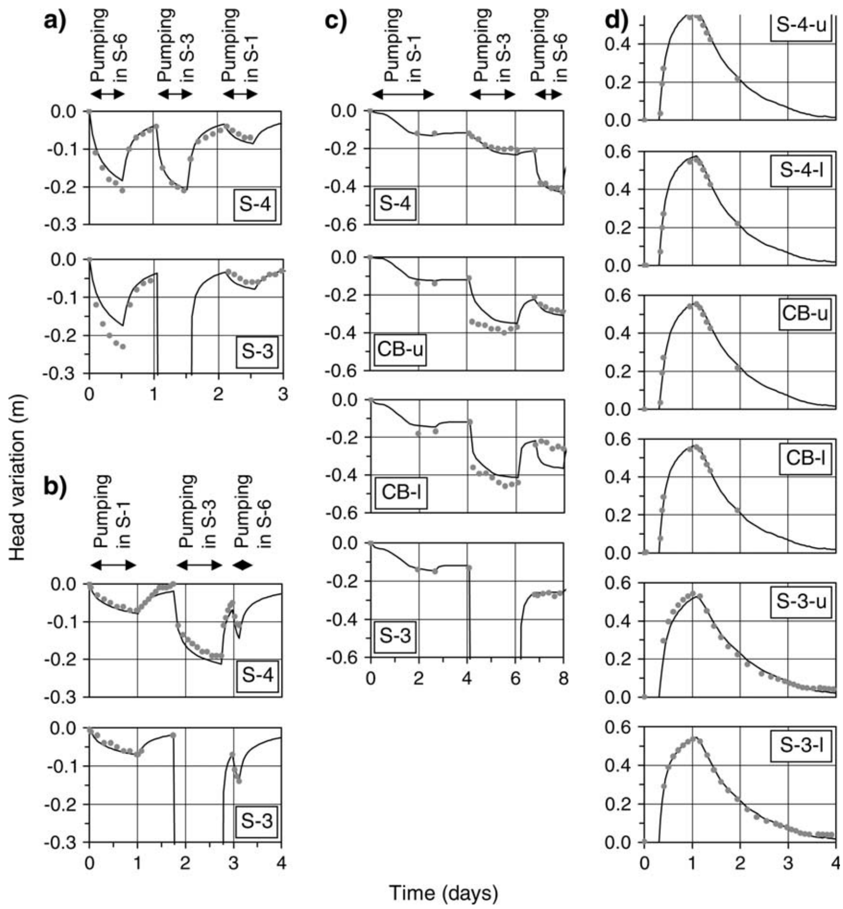

Figure 8. Measured (dots) and calculated (continuous line) head variations of model 2 in the wells of the central PRB module for (a) the first and (b) the second pumping test before PRB construction, (c) the pumping test after PRB construction, and (d) the stream-stage response test (only wells not shown in Figure 7). For clarity, not all measured data points are shown.

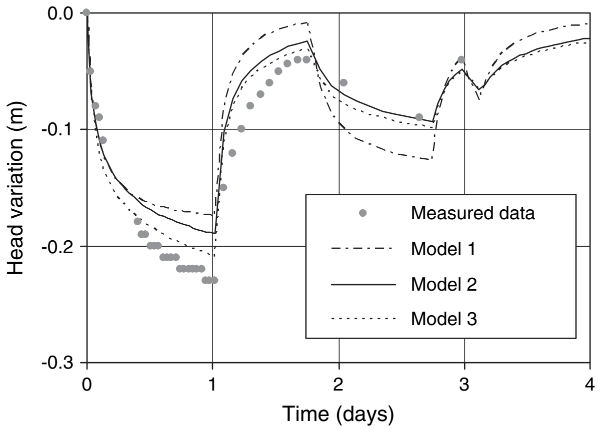

Figure 9. Measured and calculated head variations of the different model configurations in well "S-2" for the second pumping test before PRB construction.

with two exceptions: the hydraulic conductivity of the right margin barrier module of model 3 is 2 orders of magnitude lower than the prior estimate, and in the central barrier module of model 1, the hydraulic conductivities of the two K zones next to the river increase to 214 and 40 m/d, raising the geometric mean of this module to 11 m/d. In all the three models, the silt layer hydraulic conductivity is slightly lower than the prior estimate and the silt layer storage coefficient is 1 order of magnitude higher, while the remaining storage coefficients are similar to the prior values (Table 5).

Many calibrated leakances (Table 6, cf. Figure 5b) change considerably with respect to their prior estimates. In model 1, the calibrated leakance for the connection of River Agrio with the upper layer (Upper two-layer α) rises 6 orders of magnitude, while Guadiamar α drops by 1 order of magnitude. In models 2 and 3, the general patterns in the leakance zones are similar, even though actual values differ. In the two-layer zone, the highest leakance is assigned to the upper layer in 2001/2002 and a moderate value is assigned to the lower layer during the same period, while both values are lower in 2000. Upstream α in the 2001/2002 mesh is very low, while it remains almost unchanged in the 2000 mesh, as does Downstream α in both meshes. The biggest difference between the two models is found in Guadiamar α, which is lower than the prior estimate in model 2 (similar to model 1) but higher in model 3.

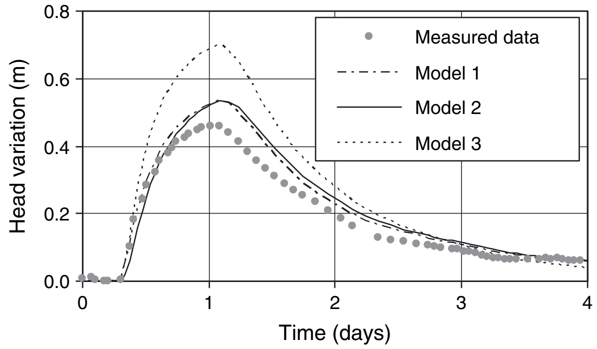

Figure 10. Measured and calculated head variations of the different model configurations in well "A-1bis" for the stream-stage response test.

Discussion

Silt Layer Continuity

The hydraulic conductivity of the silt layer is much lower than that of the upper and lower gravel layers in the three models. This shows that the models need to separate these layers hydraulically in order to reproduce the observed data. In the pumping tests (especially before the floods), the presence of the silt layer enables hydraulic pulses to pass underneath the river through the lower gravel layer, while the very good connection between the river and the upper gravel layer leads to a fast recovery after the pumping has stopped or the stream-stage peak has passed. Therefore, the silt layer seems to be a continuous feature.

Stream-Aquifer Interaction

Models 2 and 3 consistently display a marked difference between the leakances of the 2000 and the 2001/2002 meshes. In 2001/2002, they assign higher leakances than in 2000 to both layers of the two-layer zone. At least in the 2001/2002 mesh of both models, the River Agrio also has a moderate connection to the lower layer in this area. Even model 1, which was not allowed to assign a leakance to the lower-layer gravels within the two-layer zone, yields high hydraulic conductivities in two sections of the central PRB module, probably to hydraulically connect the river to the lower layer.

This shows that the winter 2000/2001 floods changed stream-aquifer interaction in this aquifer and that at least since then, the River Agrio is hydraulically connected to the lower aquifer close to the PRB. This is consistent with the observation that the River Agrio deepened and broadened its channel during the winter 2000/2001 floods. The river increased its hydraulic connection to the upper layer and probably excavated the silt layer in some parts, creating or enhancing the connection to the lower layer. As a result, pumping during the test performed after the winter 2000/2001 floods is barely noticed across the river.

Role and Geometry of the Lower Gravel Layer

Many wells at a considerable distance from the river react quickly to the stream-stage variation. This implies that (1) the gravels found beneath the western T2 terrace are well connected to the River Agrio and that (2) a confining layer exists in this part of the aquifer (low storage coefficients assigned by all models, cf. Table 5). This explanation is consistent with the silt layer continuity and river-aquifer interaction discussed previously.

As to paleochannel geometry, the proposed eastern and western boundaries can satisfactorily explain the observed data, especially the high contrast in reaction to the stream-stage response test between wells that are only

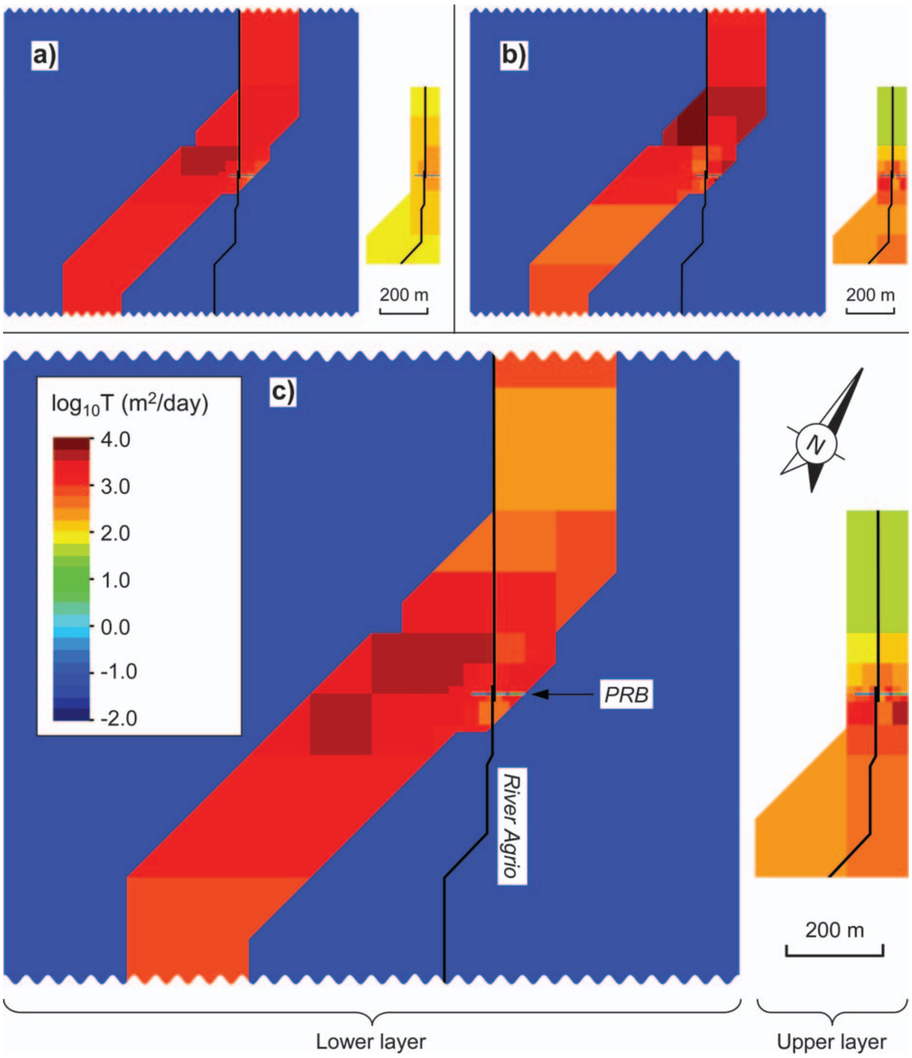

Figure 11. Transmissivity fields (left-hand side: lower layer; right-hand side: upper layer) of the geostatistical models. For the lower layer, only the central part is shown; transmissivity zones continue homogeneously up- and downstream. (a) Prior estimate of models 1 and 2. (b) Calibrated values of model 1. (c) Calibrated values of model 2.

short distances apart (Figure 7, i.e., S-26, S-24, S-28 vs. S-25, S-26 at the western border and S-5, S-6 vs. S-7 at the eastern border). At the southern end of the paleochannel, both models 1 and 2 assign a low leakance to River Guadiamar and lower paleochannel transmissivity. Model 3, which has to assign a homogeneous transmissivity to the whole paleochannel, cannot selectively lower transmissivity close to Guadiamar River. Instead, it even raises Guadiamar α, achieving fits in the wells of the southern paleochannel (S-23, S-24, S-28; not shown), which are similar to those of models 1 and 2. This seems to contradict the results of the other models,

Table 6
Prior Estimates and Calibrated Leakances (d^{-1}) for the Different Model Configurations

Leakance Zone	Prior Estimates All Models and Meshes	Model 1 Both Meshes	Model 2 2000 Mesh	Model 2 2001/2002 Mesh	Model 3 2000 Mesh	Model 3 2001/2002 Mesh
Upstream α	1.0	0.87	1.2	0.0033	0.97	0.00027
Upper two-layer α	1.0	121,200	7.6	129	0.39	24
Lower two-layer α	1.0[1]	na	0.014	7.8	0.67	5.8
Downstream α	1.0	1.0	1.0	0.99	1.0	1.0
Guadiamar α	1.0	0.098	0.088		8.1	

na = not assigned.
[1]Except model 1 (leakance zone not assigned).

but presumably, model 3 uses River Guadiamar as an injection zone (analogously to an image well) in order to imitate the effect of the low-permeability zone assigned by models 1 and 2. Therefore, we conclude that the paleochannel is only poorly connected to River Guadiamar. This conclusion is consistent with independent observations not used during modeling and not shown here. First, well S-28 was not contaminated, as it should if the paleochannel had been connected to River Guadiamar. Second, natural head gradients in the paleochannel point to the River Agrio, supporting that this area is not well connected to River Guadiamar.

Nevertheless, it is less clear how well and where the lower paleochannel is connected to River Agrio upstream of the studied area. The situation is ambiguous in two aspects. First, it appears contrary to the aforementioned theory on stream-aquifer interaction that Upstream α is higher before the winter 2000/2001 floods in models 2 and 3. This is probably only an artifact of the lack of data in this zone during the pumping tests (no measurements were taken in well A-1bis). Therefore, the models are not very sensitive to this leakance in the 2000 mesh and maintain its value close to the prior estimate. Second, none of the three model configurations achieves a satisfactory fit for well A-1bis (Figure 11). All models overestimate both peak height and peak arrival time. Additional wells and river-stage measurement points during the stream-stage response test would have helped to increase model sensitivity in this area.

Impact of PRB Construction

The PRB construction has created a low-permeability feature in the aquifer. Observation wells now react much less to pumping in wells on the opposite side of the PRB than before PRB construction. Head variations in these wells during the last pumping test series are due to changes in river stage rather than to pumping (cf. Figures 6a and 6b and 8a through 8c).

Modeling Approach

The present numerical model allows us to simultaneously interpret pumping and stream-stage response test data and to resolve aquifer diffusivities into transmissivities and storage coefficients. In our case study, the stream-stage response test alone would not reveal information about PRB characteristics because ground water flow during the stream-stage response test is parallel to the barrier.

A large number of observation points were used in the calibration. Therefore, large errors in single points lead to relatively small changes of the heads objective function. As a result, the fits have to be verified individually in all observation points in order to evaluate the conceptual model (analysis of residuals). This means that automatic calibration helps to test alternative conceptual models rapidly, but it does not eliminate the need for thorough, and often tedious, qualitative analysis of results. This applies to any model with many observation points, not only to the interpretation of stream-stage response tests.

Models 1 and 2 obtain almost equal fits for most observation points. Model 2 uses somewhat more plausible parameter values that are consistent with independent observations (changes in stream channel geometry due to the winter 2000/2001 floods) so it appears more realistic, but other models could be developed that can explain the observed data equally well.

Conclusions

A methodology for the design, execution, and joint numerical interpretation of stream-stage response tests was summarized and successfully applied to a test performed in the River Agrio (southwest Spain). The objective of the test was to complement three sets of cross-hole pumping tests in the characterization of the layered stream-aquifer system. Two geostatistical models and one "conventional" model with homogeneous transmissivities were tested in order to investigate the trade-off between model complexity and achieved fit.

The results show that

- The combination of pumping and stream-stage response test data allows calibrating both transmissivities and storage coefficients. The pumping tests yield small-scale information about the barrier and its surroundings and provide the flow data necessary to resolve diffusivity into T and S, while the stream-stage response test gives information on a larger scale.
- River-aquifer interaction can be simulated using leakances.
- The geostatistical approach obtains better overall results than the more conventional deterministic approach.
- The numerical model used in the case study allowed us to explore (1) aquitard continuity; (2) degrees and temporal changes of stream-aquifer interaction; (3) the impact of the construction of a PRB on the hydraulic system; and—to some degree—(4) aquifer geometry.

In summary, the stream-stage response test provides hydraulic information at a relatively large scale and is relatively easy to perform. Therefore, its use is recommended. However, a thorough interpretation requires coupling to pumping tests or other types of flow data, which can be achieved satisfactorily using geostatistical inversion codes.

Acknowledgments

This study was funded by the EU PIRAMID project (EVK1-1999-00061P) and by the Spanish CYCIT program (HID99-1147-C02). The authors wish to thank the Hydrographical Confederation of the Guadalquivir and C. Mediavilla from the Geological and Mining Institute of Spain in Seville for making possible the execution of the stream-stage response test, and J. Jodar and C. Knudby for their help in the initial design of the numerical model. T. Rötting's work was supported by the German Academic Exchange Service DAAD (grant number D/01/29764) and the Gottlieb-Daimler and Karl Benz Foundation (grant number 02-18/01). The authors also thank

Steffen Mehl, Marios Sophocleous, and one anonymous reviewer for their constructive comments that helped to improve the present paper.

References

Anderman, E.R., M.C. Hill, and E.P. Poeter. 1996. Two-dimensional advective transport in ground water flow parameter estimation. *Ground Water* 34, no. 6: 1001–1009.

Bolster, C.H., D.P. Genereux, and J.E. Saiers. 2001. Determination of specific yield for the Biscayne Aquifer with a canal-drawdown test. *Ground Water* 39, no. 5: 768–777.

Carrera, J., A. Alcolea, J. Bolzicco, I. Bernet, C. Knudby, M. Manzano, M.W. Saaltink, C. Ayora, C. Domenech, J. De Pablo, J.L. Cortina, G. Coscera, O. Gibert, J. Galache, A. Silgado, and R. Mantecón. 2001. An experimental geochemical barrier at Aznalcóllar. In *Groundwater Quality: Natural and Enhanced Restoration of Groundwater Pollution*. Proceedings of the Groundwater Quality 2001 Conference held at Sheffield, UK, June 2001, ed. S.F. Thornton and S.E. Oswald, 407–409. IAHS Publication 275. Wallingford, UK: IAHS Press.

Carrera, J., A. Alcolea, A. Medina, J. Hidalgo, and L.J. Slooten. 2005. Inverse problem in hydrogeology. *Hydrogeology Journal* 13, no. 1: 206–222.

Carrera, J., S.F. Mousavi, E. Usunoff, X. Sanchez-Vila, and G. Galarza. 1993. A discussion on validation of hydrogeological models. *Reliability Engineering and System Safety* 42, no. 2–3: 201–216.

Carrera, J., and S.P. Neuman. 1986a. Estimation of aquifer parameters under steady-state and transient conditions: I. Background and statistical framework. *Water Resources Research* 22, no. 2: 199–210.

Carrera, J., and S.P. Neuman. 1986b. Estimation of aquifer parameters under steady-state and transient conditions: II. Uniqueness, stability, and solution algorithms. *Water Resources Research* 22, no. 2: 211–227.

Carrera, J., and S.P. Neuman. 1986c. Estimation of aquifer parameters under steady-state and transient conditions: III. Applications. *Water Resources Research* 22, no. 2: 228–242.

Chorley, D.W., and E.O. Frind. 1978. An iterative quasi-three-dimensional finite element model for heterogeneous multiaquifer systems. *Water Resources Research* 14, no. 5: 943–952.

Cooper, H.H., and M.I. Rorabaugh. 1963. Groundwater movements and bank storage due to flood stages in surface stream. USGS Water Supply Paper 1536-J. USGS, Reston, Virginia.

Crank, J. 1975. *The Mathematics of Diffusion*, 2nd ed. Oxford, UK: Clarendon Press.

Erskine, A.D. 1991. The effect of tidal fluctuation on a coastal aquifer in the UK. *Ground Water* 29, no. 4: 556–562.

Ferris, J.G. 1951. Cyclic fluctuations of water level as a basis for determining aquifer transmissibility. In *Proceedings of the International Union of Geodesy and Geophysics*, 148–155. IAHS Publication 33. IAHS, Louvain.

Genereux, D.P., and J. Guardiario. 1998. A canal drawdown experiment for determination of aquifer parameters. *Journal of Hydraulic Engineering* 3, no. 4: 294–302.

Grimalt, J.O., M. Ferrer, and E. Macpherson. 1999. The mine tailing accident in Aznalcollar. *The Science of the Total Environment* 242, no. 1–3: 3–11.

Grubb, H.F., and H.H. Zehner. 1973. Aquifer diffusivity of the Ohio River alluvial aquifer by the floodwave response method. *U.S. Geological Survey Journal of Research* 1, no. 5: 597–601.

Hantush, M.S. 1961. Discussion of “An equation for estimating transmissibility and coefficient of storage from river-level fluctuations” by P.P. Rowe. *Journal of Geophysical Research* 66, no. 4: 1310–1311.

Hill, M.C., R.L. Cooley, and D.W. Pollock. 1998. A controlled experiment in ground water flow model calibration. *Ground Water* 36, no. 3: 520–535.

Hornberger, G.M., J. Ebert, and I. Remson. 1970. Numerical solution of Boussinesq equation for aquifer-stream interaction. *Water Resources Research* 6, no. 2: 601–610.

Jha, M.K., Y. Kamii, and K. Chikamori. 2003. On the estimation of phreatic aquifer parameters by the tidal response technique. *Water Resources Management* 17, no. 1: 69–88.

Kashyap, R.L. 1982. Optimal choice of AR and MA parts in autoregressive moving average models. *IEEE Transactions on Pattern Analysis and Machine Intelligence* 4, no. 2: 99–104.

Liu, S.Y., T.C.J. Yeh, and R. Gardiner. 2002. Effectiveness of hydraulic tomography: Sandbox experiments. *Water Resources Research* 38, no. 4, 1034.

Loeltz, O.J., and S.A. Leake. 1983. A method for estimating groundwater return flow to the lower Colorado river in the Yuma Area. USGS Water Resources Investigation Report 83-4220. USGS, Tucson, Arizona.

Medina, A., G. Galarza, and J. Carrera. 1995. *TRANSIN-II, FORTRAN Code for Solving the Coupled Flow and Transport Inverse Problem. User's Guide*. Barcelona, Spain: Universitat Politecnica de Catalunya.

Meier, P., A. Medina, and J. Carrera. 2001. Geostatistical inversion of cross-hole pumping tests for identifying preferential flow channels within a shear zone. *Ground Water* 39, no. 1: 10–17.

Mishra, G.C., and S.K. Jain. 1999. Estimation of hydraulic diffusivity in stream-aquifer system. *Journal of Irrigation and Drainage Engineering* 125, no. 2: 74–81.

Moench, A.F., and P.M. Barlow. 2000. Aquifer response to stream-stage and recharge variations. I. Analytical step-response functions. *Journal of Hydrology* 230, no. 3–4: 192–210.

Onder, H. 1997. Analysis of one-dimensional ground-water flow in a nonuniform aquifer. *Journal of Hydraulic Engineering* 123, no. 8: 732–736.

Pinder, G.F., J.D. Bredehoeft, and H.H. Cooper. 1969. Determination of aquifer diffusivity from aquifer response to fluctuations in river stage. *Water Resources Research* 5, no. 4: 850–855.

Poeter, E.P., and M.C. Hill. 1997. Inverse models: A necessary next step in ground water modeling. *Ground Water* 35, no. 2: 250–260.

Reynolds, R.J. 1987. Diffusivity of a glacial-outwash aquifer by the floodwave-response-technique. *Ground Water* 25, no. 3: 290–298.

Rorabaugh, M.I. 1960. Use of water levels in estimating aquifer constants in a finite aquifer. *International Association of Scientific Hydrology Publication* 52, 314–323.

Rowe, P.P. 1960. An equation for estimating transmissibility and coefficient of storage from river-level fluctuations. *Journal of Geophysical Research* 65, no. 10: 3419–3424.

Saiers, J.E., D.P. Genereux, and C.H. Bolster. 2004. Influence of calibration methodology on ground water flow predictions. *Ground Water* 42, no. 1: 32–44.

Salvany, J.M., J. Carrera, J. Bolzicco, and C. Mediavilla. 2004. Pitfalls in the geological characterization of alluvial deposits: Site investigations for reactive barrier installation at Aznalcóllar, Spain. *Quarterly Journal of Engineering Geology and Hydrogeology* 37, no. 2: 141–154.

Sanchez-Vila, X., J. Carrera, and J.P. Girardi. 1996. Scale effects in transmissivity. *Journal of Hydrology* 183, no. 1–2: 1–22.

Singh, S.K. 2003. Explicit estimation of aquifer diffusivity from linear stream stage. *Journal of Hydraulic Engineering* 129, no. 6: 463–469.

Singh, S.R., and B. Sagar. 1977. Estimation of aquifer diffusivity in stream-aquifer systems. *Journal of the Hydraulics Division* 103, no. 11: 1293–1302.

Snodgrass, M.F., and P.K. Kitanidis. 1998. Transmissivity identification through multi-directional aquifer stimulation. *Stochastic Hydrology and Hydraulics* 12, no. 5: 299–316.

Sophocleous, M.A. 2002. Interactions between groundwater and surface water: The state of the science. *Hydrogeology Journal* 10, no. 1: 52–67.

Sophocleous, M.A. 1991. Stream-floodwave propagation through the Great Bend alluvial aquifer, Kansas: Field measurements and numerical simulations. *Journal of Hydrology* 124, no. 3–4: 207–228.

Swamee, P.K., and S.K. Singh. 2003. Estimation of aquifer diffusivity from stream stage variation. *Journal of Hydrologic Engineering* 8, no. 1: 20–24.

Tabidian, M.A., D. Pederson, and P.A. Tabidian. 1992. A paleovalley aquifer system and its interaction with the Big Blue River of Nebraska during a major flood. In *The Future Availability of Ground Water Resources*, ed. R.C. Borden and W.L. Lyke, 165–172. Raleigh, North Carolina: American Water Resources Association.

Weiss, R., and L. Smith. 1998. Parameter space methods in joint parameter estimation for groundwater flow models. *Water Resources Research* 34, no. 4: 647–661.

Yeh, T.-C.J., and S.Y. Liu. 2000. Hydraulic tomography: Development of a new aquifer test method. *Water Resources Research* 36, no. 8: 2095–2105.

Zlotnik, V.A., and H. Huang. 1999. Effect of shallow penetration and streambed sediments on aquifer response to stream stage fluctuations (analytical model). *Ground Water* 37, no. 4: 599–605.